



ELSEVIER

1 December 2000

OPTICS
COMMUNICATIONS

Optics Communications 186 (2000) 1–14

www.elsevier.com/locate/optcom

Method for measurement of the directional/hemispherical reflectance of photovoltaic devices

A. Parretta^{a,*}, P. Grillo^{a,1}, P. Maddalena^{b,2}, P. Tortora^{b,2}

^a ENEA Centro Ricerche, Località Granatello, C.P. 32, I-80055 Portici, Napoli, Italy

^b INFN, Dip. Scienze Fisiche, Università Federico II di Napoli, 80126 Napoli, Italy

Received 5 June 2000; accepted 2 October 2000

Abstract

A novel method, and the relative apparatus, are described which permit to measure the directional/hemispherical reflectance of a surface at incidence angles θ in the interval $0\text{--}90^\circ$. The method, suitable for the characterization of optically homogeneous as well as heterogeneous samples, is named “differencing reflection method” as the reflectance of the sample, $R_{\text{dh}}(\theta, \lambda)$, is derived from differences among the reflectance signal measured for the sample and those measured for two diffuse reflectance standards. In order to be applied, the method requires the knowledge of the directional/hemispherical reflectance of the standards for the wavelength range of interest and for incidence angle interval $0\text{--}90^\circ$. The method has been applied to measurements of $R_{\text{dh}}(\theta, \lambda)$ of solar cells. © 2000 Elsevier Science B.V. All rights reserved.

1. Introduction

The optical characterization of photovoltaic (PV) devices, aimed at evaluating their optical losses, is commonly performed by commercial spectrophotometers. Typical measurements are the directional/hemispherical (total and diffuse) re-

flectance, $R_{\text{dh}}(\theta, \lambda)$, of these samples at $\theta \approx 8^\circ$ of incidence and as a function of the wavelength. An angle of incidence $\theta \approx 8^\circ$ is close to $\theta \approx 0^\circ$, which is one of the five standard conditions (standard test conditions (STC) [1]) defined for the testing of PV devices. To better investigate the light collection and trapping properties of these devices, it is useful to know their directional/hemispherical reflectance also at incidence angles different from the STC value, as this condition is met in practice, when the PV device is installed outdoors. A procedure for the measurement of the solar or photopic reflectance of materials at incidence angles up to 60° , by using large diameter integrating spheres, is described in Ref. [2]. Other procedures have been developed by us [3–5] to measure $R_{\text{dh}}(\theta, \lambda)$ (both total and diffuse) of PV

* Corresponding author. Tel.: +39-81-7723262; fax: +39-81-7723344.

E-mail addresses: parretta@portici.enea.it (A. Parretta), pasmad@na.infn.it (P. Maddalena).

¹ Tel.: +39-81-7723262; fax: +39-81-7723344.

² Tel.: +39-81-676126; fax: +39-81-676346.

materials and devices at incidence angles well above 60° .³

In all these angle-dependent reflectance methods, a collimated light beam illuminates a small region of the sample surface (see Fig. 1a). By increasing θ , the illuminated area increases, reaching the edges of the sample at a limiting value, θ_L , above which the measurements lose significance (see Fig. 1b). Due to the variation with the angle of the illuminated area, moreover, the measurements become incompatible when the sample is optically heterogeneous.

These two limiting conditions have been fully overcome by the present method [6]. By using the optical apparatus described in this paper, the measurements can be performed on samples with dimensions of the order of few centimetres, at different wavelengths of the incident light. Measurements are not limited, in principle, to this sample size, because larger samples can be characterized realizing a different apparatus with a larger integrating sphere, a larger sample holder, and so on. Due to the peculiar procedure followed to get the hemispherical reflectance, the method has been named differencing reflection method (DRM). The DRM permits to measure the hemispherical reflectance at these conditions: (i) the incidence angle can be varied from 0° to 90° ; (ii)

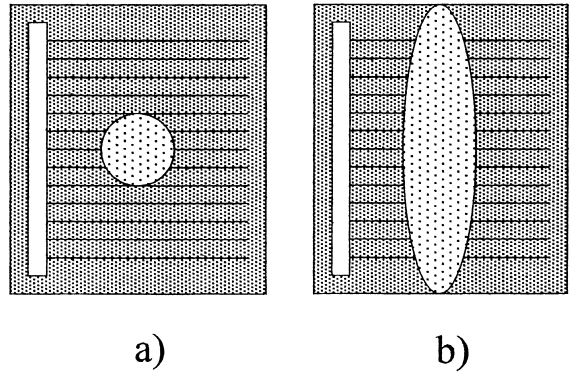


Fig. 1. It is shown the light spot appearing on the surface of a solar cell at different incidence angles of the light beam: a) $\theta = 0^\circ$ and b) $\theta = \theta_L$.

the entire selected surface of the sample is homogeneously illuminated. Besides the points (i) and (ii), the DRM shows the considerable practical advantage that spectral measurements are easily performed by using a white light lamp. When high values ($80\text{--}85^\circ$) of the angle θ have to be reached, in fact, the former methods [3–5] require the use of a laser light source, that assures the illumination of a very small area of the sample surface at 0° incidence. To vary the light wavelength, therefore, it is necessary either to change the laser source itself or to use tunable lasers. Continuous variations of the wavelength are then difficult and unpractical to perform. By the DRM apparatus, on the contrary, it is not necessary to reduce the cross-section of the beam to reach high θ values, because a collimated beam of some centimetres cross-section is required, and then less expensive optical components can be used to carry out the spectral measurements.

The optical reflectance characterization of PV devices, by both the old [3–5] and the new [6] methods, generally presents the drawback that a small portion of the incident light is reflected by the metal grid, when it is used for the front contact, e.g. in monocrystalline silicon (mono-Si) and multicrystalline silicon (m-Si) solar cells. The reflection of light from the grid is unavoidable when the DRM method is used, as the selected area for the measurements is large enough to let both the semiconductor (or optically active, o.a.) and the grid area exposed to light. On these conditions,

³ The procedures described in Refs. [3–5] are based on the use of a reflectometer named reflectometer for optical measurements in solar energy (ROSE), which permits the optical characterization (reflectance, transmittance) of both small samples (solar cells, solar energy materials) [5] and large samples (PV modules, large glass sheets) [4]. The reflectometer is equipped with a 40 cm in diameter integrating sphere provided with multiple ports for the input of light and the extraction of the beam specularly reflected by the sample, when necessary. The multiple ports permit to change the incidence angle of the light beam when samples of large dimensions (>7 cm), impossible to insert into the sphere, are to be characterized. The large samples are faced to one window of the sphere and are characterized by changing the incidence of the light beam from 0° to 70° with 10° steps. Small samples are positioned at the centre of the sphere, and characterized pointing the input beam towards the 0° port and rotating the sample holder in a continuous way. The incidence angle can be varied, in this case, from 0° to $70\text{--}80^\circ$, if a lamp light source is used. By using laser sources it is possible to reach θ values very close to 90° .

the resulting reflectance data have to be corrected in order to remove the contribution given by the metal grid and to obtain the reflectance of only the o.a. area, $R_{o.a.}(\theta)$. Some formulae have been reported in our previous works [4,5] to correct the experimental reflectance data. They have been applied to measurements on PV modules [4], where the cell is covered by the encapsulant and the glass sheet, and directly on unencapsulated solar cells [5].

2. The basic differencing reflection method apparatus

The basic DRM apparatus, in the configuration for spectral reflectance measurements, is schematically represented in Fig. 2. It consists of a light source (s), an integrating sphere (is) and a radiation detection system (r) + (v). The light source (s) provides with a parallel, white light beam. The integrating sphere, depending on the size of the tested samples and on the precision required for the measurements, can have a diameter in the 20–40 cm range. As will be better described in the following paragraphs, a larger sphere diameter assures a higher precision of measurements at high angles of incidence. The detection system consists of a silicon photodiode (r) and a voltmeter or lock-in (v). The lock-in measures the current of the photodiode, which is linearly dependent on the

irradiance inside the sphere. The lock-in configuration permits a higher sensitivity of light measurements, but requires the chopping of light from the source (s). A continuous light beam in the sphere can also be used and, in this case, the photodiode can be connected to a resistive load of 100–1 k Ω , and (v) can represent a digital voltmeter. The sample (c) is inserted in a black box (b) (see Fig. 3), that is fixed at one end of the sample holder (p). The box is provided with a small window, where the sample is faced to, from the inside of the box, exposing a selected area, S_0 , of the sample surface. Acting on the head (h) of the sample holder (p), the sample can be rotated around the vertical axis (y). The angle by which the sample holder is rotated can be read on a goniometer installed on the window (w3). The sample holder (p) should be made of a highly reflective rod in order to not contribute to absorb the light collected by the sphere, and then to keep high the level of the irradiation inside it. The box (b), containing the sample (c) or a diffuse reflectance standard, should be painted by a black coating in order to reflect as little as possible the light incident on its surface. This condition is not strictly necessary as the method, based on differences between irradiation measurements, is able to remove the contribution given by the box to the light reflected into the sphere. However, less reflective is the box surface, better is for the signal to noise ratio. The sphere (is) is provided with two windows

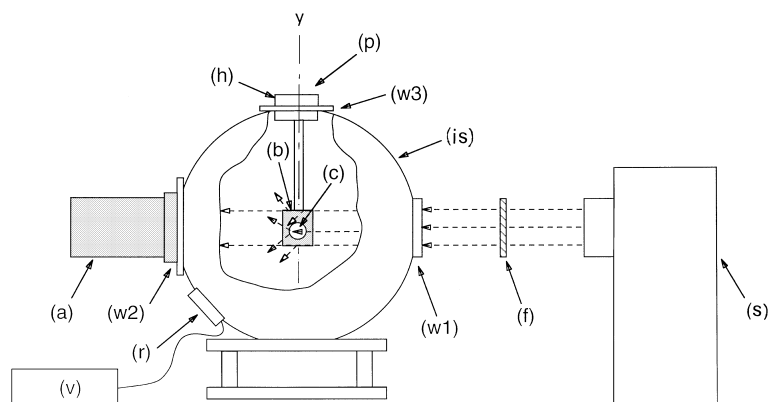


Fig. 2. Schematic of the basic DRM apparatus with the sample lowered to intercept the collimated light beam at the centre of the integrating sphere.

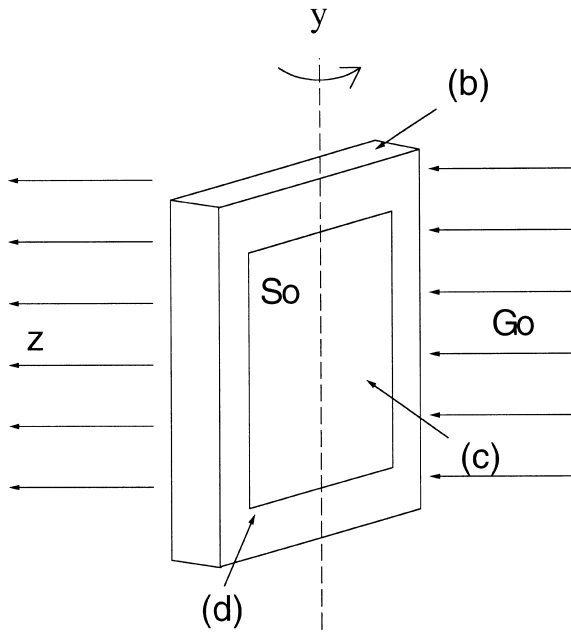


Fig. 3. Drawing of the box containing the test sample (c). The window (d) exposes to light a selected portion, of area S_0 , of the sample surface. In the figure, the light is incident at an angle θ .

(w1) and (w2), diametrically opposed, and with a black cylinder (a) which acts as a light absorber. The filter (f) is used to select a narrow band of wavelengths. The DRM reflectance measurements need a preparation of the light beam which consists in holding up the sample (c), in directing the parallel beam towards the absorber, through the two windows (w1) and (w2), and in checking the light into the sphere being as low as possible. The beam cross-section has to be smaller than the windows (w1) and (w2), and the irradiance inside the sphere has to be minimized in these conditions, as all the light must be absorbed by the cylinder (a). When the sample holder (p) is lowered (see Fig. 2) the sample lies at the centre of the sphere and its whole surface is illuminated together with a portion of the box surface. The sample holder (p) can be rotated around the vertical axis (y) in such a way to vary the incidence angle continuously from 0° to 90° . In Fig. 2 it can be seen that all the selected area of the sample and a portion of the box surface are illuminated by the beam and they will reflect a fraction of the incident beam inside the sphere. Due to the

low reflectivity of (b), however, most of the reflected light comes from the sample (c). The light collected by the sphere is measured by the detector (r), which gives a current proportional to the irradiance on the internal wall of the sphere. By comparing the irradiance measured on the sample (c), at different θ values, with that measured on two standards of diffuse reflectance, it is possible, as it will be hereafter explained, to deduce the reflectance, $R_{\text{dh}}(\theta, \lambda)$, of the sample (c).

The method, therefore, gives the total hemispherical reflectance of a plane surface, as function of the incidence angle from 0° to 90° . The illuminated area of (c) is constant, at the different θ values, and corresponds to the area S_0 of the box window (see Fig. 3). The measured reflectance always refers to the same region of the sample (c). The method proves to be indispensable when dealing with optically heterogeneous samples, as generally are PV materials and devices. The reflectance measurements have to be corrected for the effect of the metal grid, when it is present, as discussed in Section 1.

3. Experimental

Fig. 4a shows the photo of the DRM apparatus, assembled on an optical bench, as realized in our laboratory. It is configured for spectral measurements, in particular for measurements with a light beam having a narrow (few tenths of nanometers) distribution in wavelength. On the left side of the photo, it is shown a He–Ne laser, and the relative optics, that can be used as light source as an alternative to the lamp. Fig. 4b shows a particular of the optics of the apparatus. The details of the apparatus are also reported in Fig. 5.

The apparatus uses a 40 cm in diameter integrating sphere (ROSE), already employed by us in other optical measurements on solar cells and PV modules [3–5]. The light source is a 250 W Oriel quartz tungsten halogen (QTH) lamp. The collimated white-light beam of the lamp is focused by the lens (l_1) on the filter (f), then chopped by the mechanical chopper (ch) and collimated again at the input of the sphere by the lens (l_2). In Fig. 5a (d1)–(d4) are diaphragms. The filter (f) is a 70-nm

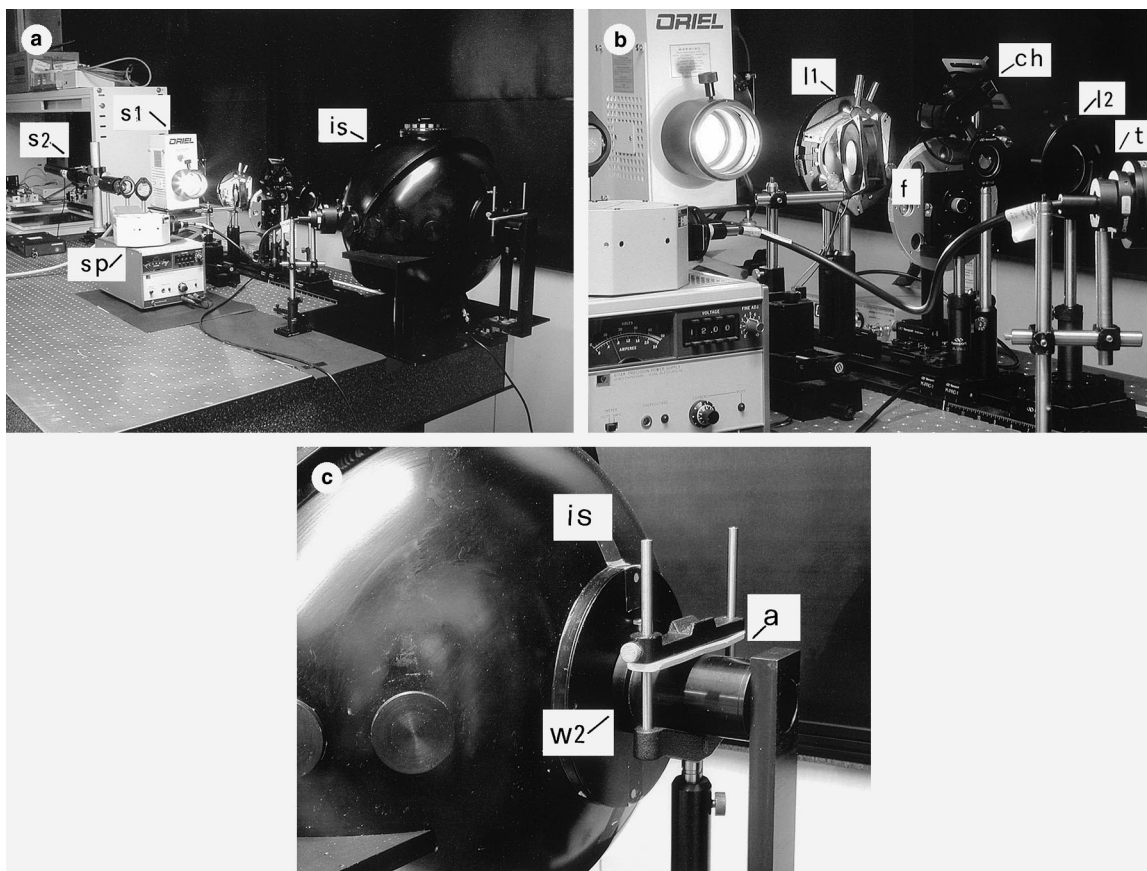


Fig. 4. (a) Photograph of the DRM apparatus configured for spectral measurements. On the left side is placed a laser source, and the relative optics, as an alternative to the lamp (see also Fig. 5). (b) Particular of the apparatus with the optical components. (c) Back side of the integrating sphere, with the absorber (a) mounted on the (w2) window.

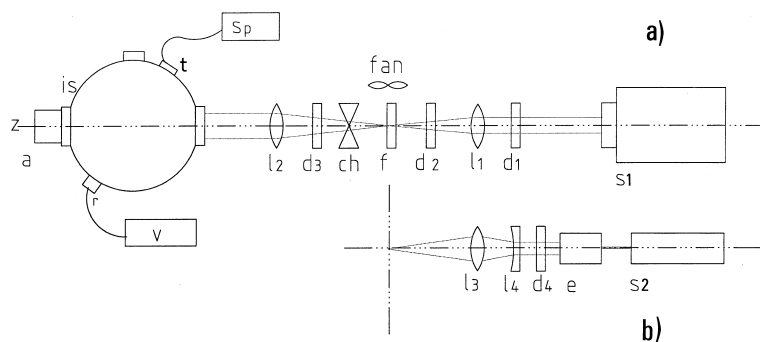


Fig. 5. Experimental set-up of the DRM apparatus for spectral measurements: (a) lamp source; (b) laser source.

nominal bandwidth Corion interferential filter and is cooled by a fan. Only filters with nominal central

wavelengths 50 nm apart were used (e.g. 600, 650, 700 nm etc.). The absorber (a) was made by a

4.5 cm in diameter cylinder, with the internal surface coated with a black, highly absorbing coating. A particular of the back side of the sphere, with the absorber (b) mounted on the (w2) window, is shown in Fig. 4c. The light spectrum inside the sphere was measured by using the Oriel InstaSpec II PDA Spectrograph equipped with an Oriel Multispec monochromator (600 l/mm reticle).

For white-light reflectance measurements with spectrum s , $R_C(\theta, s)$, the silicon photodiode (r) must be replaced by a pyroelectric detector, as a detector with a flat spectral response is indispensable for this type of measurements. Due, moreover, to the lower sensitivity of this type of detectors respect to photodiodes, the use of the lock-in configuration is strictly necessary. For white-light measurements, it can be used a 250 W Oriel Xe arc lamp as light source and, as light detector system, the Laser Precision Rk-5720 Power Radiometer, equipped with the RkP-575 pyroelectric detector. Xe arc lamps emit light with a spectrum similar to that of the solar radiation, apart from some peaks typical of the Xe ions emissions. In this case, the white-light reflectance measurement directly gives the reflectance the PV device should manifest in outdoors when exposed to the direct solar radiation.

The DRM measurements can also be performed at strictly monochromatic light by using a laser as light source (see Figs. 4a and 5b). The use of a laser requires the expansion of the beam by a beam expander (e), in order to produce a collimated light with an appropriate cross-section at the input of the sphere. Fig. 5b shows how the configuration of the apparatus changes in the light source section when a laser source is employed.

Fig. 6 shows a photo of the black box (b) containing a solar cell and the white-painted sample holder rod. The front side of the box was built by using a metal sheet of ≈ 0.5 mm thickness. The entire external surface of the box (b) was given a coat of black, opaque paint, to reduce at minimum its reflectance. The use of a highly light absorbing coating for the box surface is not strictly necessary, as previously discussed, as the DRM method is based on differencing measurements that, in principle, should completely eliminate the reflection signal produced by the box surface. In practice, it is convenient to coat the box by a black coating to reduce the background light and to improve the signal to noise ratio.

The standard measurements of reflectance carried out at $\theta = 0-90^\circ$, following the method reported in Refs. [3–5], and used as a comparison

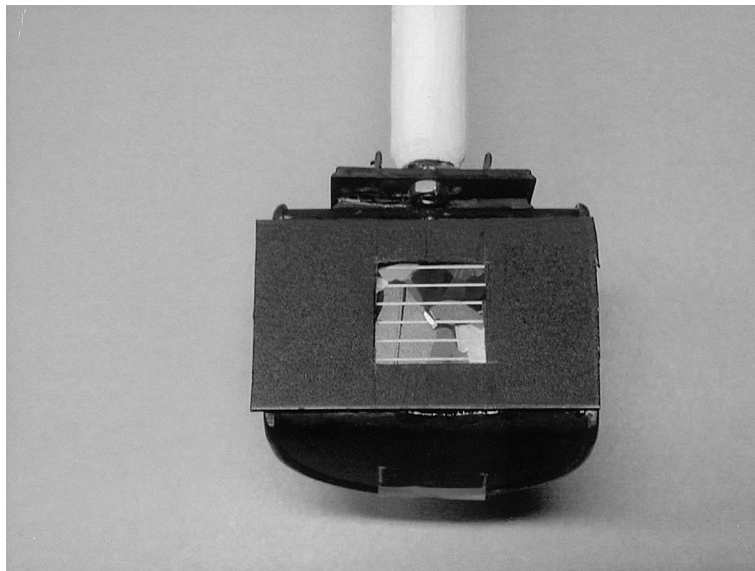


Fig. 6. Photograph of the box (b) containing a solar cell.

with the new DRM measurements in order to validate these last ones (see Section 5), were performed by using the ROSE apparatus equipped with an Oriel He–Ne laser source operating at $\lambda = 633$ nm and with a 20 mW power of unpolarized light.

Both the old and the DRM measurements were carried out using, as references, diffuse reflectance standards from Labsphere, having different nominal 8°/hemispherical reflectance. Besides the white standard, made of pure Spectralon material (a Teflon based polymer) and showing a $\geq 99\%$ hemispherical reflectance, the diffuse gray standards used by us are obtained by blending different kinds of pigments with the white Spectralon. This operation reduces the high lambertian character of the white Spectralon [7]. As a consequence, the hemispherical reflectance of the gray standards will not be perfectly constant with the angle, as will be shown later and as has been reported in Ref. [8].

4. Principles of differencing reflection method

The DRM is based on a relatively simple procedure, which consists in the measurement of the irradiance inside the integrating sphere, at different incidence angles θ , for the unknown sample and for two standards of diffuse reflectance, whose reflectance values should preferentially be close to that of the sample under test.

Figs. 3 and 6 show the box (b), inside which the sample (c) is placed, facing the window (d), from the inside of the box, in such a way to expose to light a fixed area, S_0 . A collimated light beam, of irradiance G_0 and wavelength λ , or spectrum s , is directed along the z axis and is supposed homogeneous on a plane orthogonal to z . The box can be rotated around the y axis and then the sample can be oriented at a particular angle of incidence θ respect to the z direction.

4.1. Spectral reflectance

The principles of the method are described in the following for the case of monochromatic light. The same concepts apply to the case of a source

light distributed over a narrow band of wavelengths.

If G_0 is the irradiance produced by the light source at the sample location, then the irradiance on the sample (c) becomes (the wavelength is omitted here for simplicity):

$$G(\theta) = G_0 \cos \theta \quad (\text{W/m}^2) \quad (1)$$

The light power incident on the sample, $P_{1C}(\theta)$, is given by:

$$P_{1C}(\theta) = G(\theta)S_0 = G_0 \cos \theta S_0 \quad (\text{W}) \quad (2)$$

where S_0 is the illuminated area of the sample, that is the area of the window (d) of the box (see Figs. 3 and 6). It is here supposed negligible the shadowing effect produced by the edge of window (d) on the sample surface.

If $R_C(\theta)$ is the sample reflectance, the light power reflected into the sphere by the sample is:

$$P_C(\theta) = R_C(\theta)P_{1C}(\theta) = R_C(\theta)G_0 \cos \theta S_0 \quad (3)$$

In presence of the box with reflectance $R_B(\theta)$, the total light power reflected into the sphere becomes:

$$P_{BC}(\theta) = R_C(\theta)P_{1C}(\theta) + R_B(\theta)P_{1B}(\theta) \quad (4')$$

where the “C” and “B” indices refer to the sample and the box, respectively. In presence of a standard of reflectance $R_S(\theta)$, the total light power reflected into the sphere becomes:

$$P_{BS}(\theta) = R_S(\theta)P_{1C}(\theta) + R_B(\theta)P_{1B}(\theta) \quad (4'')$$

Differencing Eqs. (4') and (4''), we obtain:

$$\begin{aligned} \Delta P_{CS}(\theta) &= P_{BC}(\theta) - P_{BS}(\theta) \\ &= P_{1C}(\theta)[R_C(\theta) - R_S(\theta)] \end{aligned} \quad (5)$$

Following Eq. (5), the sample reflectance becomes:

$$\begin{aligned} R_C(\theta) &= R_S(\theta) + \frac{\Delta P_{CS}(\theta)}{P_{1C}(\theta)} \\ &= R_S(\theta) + \frac{\Delta P_{CS}(\theta)}{[G_0 \cos \theta S_0]} \end{aligned} \quad (6)$$

The sample reflectance $R_C(\theta)$, therefore, can be obtained, in principle, by using only one standard, if the irradiance of the light beam, G_0 , is measured. In practice, a great simplification in the measurement of $R_C(\theta)$ is obtained following a procedure by which two measurements on two different

standards are carried out, besides that on the sample. We define $V(\theta)$ as the signal (in volts on the voltmeter, or in amperes on the lock-in) corresponding to a generic measurement (where both the voltmeter and the lock-in being indicated as (v) in Figs. 2 and 3). The measurement on a standard of diffuse reflectance will give:

$$V_S(\theta) = kG_0[R_B(\theta)S_B(\theta) + R_S(\theta)S_S(\theta)] \quad (\text{volts or amperes}) \quad (7)$$

where k is a proportionality factor between the power of light, at wavelength λ , collected by the sphere and the signal measured by (v); $S_B(\theta)$ is the box cross-section, namely the projection of the box surface on a plane orthogonal to the incident beam.

Being the box surface not planar, $S_B(\theta)$ will be a complex function of θ , but this is irrelevant as this quantity does not appear in the final formulae. Being, on the contrary, the standard surface planar, the cross-section of the standard, $S_S(\theta)$, will simply be:

$$S_S(\theta) = S_S(0^\circ) \cos \theta = S_0 \cos \theta \quad (8)$$

By carrying out two measurements with the standards S_1 and S_2 , we have:

$$V_{S_1}(\theta) = kG_0[R_B(\theta)S_B(\theta) + R_{S_1}(\theta)S_{S_1}(\theta)] \quad (9')$$

$$V_{S_2}(\theta) = kG_0[R_B(\theta)S_B(\theta) + R_{S_2}(\theta)S_{S_2}(\theta)] \quad (9'')$$

Differencing Eqs. (9') and (9''), we obtain:

$$\begin{aligned} \Delta V_S &= V_{S_2}(\theta) - V_{S_1}(\theta) \\ &= kG_0[R_{S_2}(\theta)S_{S_2}(\theta) - R_{S_1}(\theta)S_{S_1}(\theta)] \end{aligned} \quad (10)$$

The unknown quantities, $R_B(\theta)$ and $S_B(\theta)$, have been in this way eliminated. The measurement on the unknown sample now gives:

$$V_C(\theta) = kG_0[R_B(\theta)S_B(\theta) + R_C(\theta)S_C(\theta)] \quad (9''')$$

where $S_C(\theta)$ is the surface area of the sample exposed to light on a plane orthogonal to the z axis.

Differencing Eqs. (9') and (9'''), we obtain:

$$\begin{aligned} \Delta V_C &= V_C(\theta) - V_{S_1}(\theta) \\ &= kG_0[R_C(\theta)S_C(\theta) - R_{S_1}(\theta)S_{S_1}(\theta)] \end{aligned} \quad (10')$$

Dividing Eq. (10') by Eq. (10), we obtain:

$$\begin{aligned} \frac{\Delta V_C}{\Delta V_S} &= \frac{[V_C(\theta) - V_{S_1}(\theta)]}{[V_{S_2}(\theta) - V_{S_1}(\theta)]} \\ &= \frac{[R_C(\theta)S_C(\theta) - R_{S_1}(\theta)S_{S_1}(\theta)]}{[R_{S_2}(\theta)S_{S_2}(\theta) - R_{S_1}(\theta)S_{S_1}(\theta)]} \end{aligned} \quad (11)$$

As the surface exposed to light, on a plane orthogonal to the z axis, is the same for all the samples, we have:

$$S_C(\theta) = S_{S_1}(\theta) = S_{S_2}(\theta) = S_0 \cos \theta \quad (8')$$

and Eq. (11) becomes:

$$\frac{\Delta V_C}{\Delta V_S} = \frac{[R_C(\theta) - R_{S_1}(\theta)]}{[R_{S_2}(\theta) - R_{S_1}(\theta)]} \quad (11')$$

Finally, we have for the unknown reflectance, including the wavelength dependence:

$$R_C(\theta, \lambda) = \frac{\Delta V_C}{\Delta V_S} [R_{S_2}(\theta, \lambda) - R_{S_1}(\theta, \lambda)] + R_{S_1}(\theta, \lambda) \quad (11'')$$

By knowing the reflectance $R_S(\theta, \lambda)$ of the two standards, therefore, the sample reflectance, $R_C(\theta, \lambda)$, can be derived by Eq. (11''). Generally, as already discussed, only the $R_S(8^\circ, \lambda)$ reflectance is known by the calibration charts of the standard. For ideal diffuse reflectors, we expect that $R_S(\theta, \lambda) = R_S(8^\circ, \lambda) = \text{constant}$ [7]. In reality, $R_S(\theta, \lambda)$ is not constant with the angle [8], and then it must be measured precisely, by adopting one of the methods described in [3–5,8].

4.2. White-light reflectance

Measurements at white-light are particularly useful in the PV field, if the spectrum of the light source matches that of the direct solar irradiation, as, in this case, the measured reflectance directly gives the absolute optical loss of the PV device exposed to the light of the solar disk.

If the spectral irradiance of the light, on a plane orthogonal to the beam direction and at the sample location, is $G_S(0^\circ, \lambda)$, we have for the spectral irradiance on the sample at incidence θ :

$$G_S(\theta, \lambda) = G_S(0^\circ, \lambda) \cos \theta \quad (12)$$

and for the total irradiance:

$$\begin{aligned}
 G_S(\theta) &= \int d\lambda G_S(\theta, \lambda) \\
 &= \cos\theta \int d\lambda G_S(0^\circ, \lambda) \quad (13)
 \end{aligned}$$

The light power on the sample (c) becomes:

$$\begin{aligned}
 P_C(\theta, s) &= G_S(\theta)S_0 \\
 &= S_0 \cos(\theta) \int d\lambda G_S(0^\circ, \lambda) \quad (14)
 \end{aligned}$$

If $R_C(\theta, \lambda)$ is the angle-resolved spectral reflectance of the sample, then we have for the angle-resolved reflectance at light of spectrum s :

$$\begin{aligned}
 R_C(\theta, s) &= \frac{\int d\lambda R_C(\theta, \lambda)G_S(\theta, \lambda)}{\int d\lambda G_S(\theta, \lambda)} \\
 &= \frac{\int d\lambda R_C(\theta, \lambda)G_S(0^\circ, \lambda)}{\int d\lambda G_S(0^\circ, \lambda)} \quad (15)
 \end{aligned}$$

An equivalent expression applies for the reflectance of the standards:

$$\begin{aligned}
 R_S(\theta, s) &= \frac{\int d\lambda R_S(\theta, \lambda)G_S(\theta, \lambda)}{\int d\lambda G_S(\theta, \lambda)} \\
 &= \frac{\int d\lambda R_S(\theta, \lambda)G_S(0^\circ, \lambda)}{\int d\lambda G_S(0^\circ, \lambda)} \quad (15')
 \end{aligned}$$

The reflected light power from the sample (c) becomes:

$$\begin{aligned}
 P_C(\theta, s) &= \int d\lambda P_C(\theta, \lambda) \\
 &= \int d\lambda R_C(\theta, \lambda)S_0 G_S(\theta, \lambda) \\
 &= \int d\lambda R_C(\theta, \lambda)S_0 \cos\theta G_S(0^\circ, \lambda) \quad (16)
 \end{aligned}$$

Being the spectral response of the detector flat, the proportionality factor of Eq. (7), k , is constant with the wavelength and the measured signal becomes:

$$V_C(\theta, s) = \int d\lambda kP_C(\theta, \lambda) = kP_C(\theta, s) \quad (17)$$

The formulae found for the angle-resolved spectral reflectance can be applied also to the angle-resolved, white-light reflectance:

$$R_C(\theta, s) = \frac{\Delta V_C}{\Delta V_S} [R_{S_2}(\theta, s) - R_{S_1}(\theta, s)] + R_{S_1}(\theta, s) \quad (18)$$

where:

$$\Delta V_C = V_C(\theta, s) - V_{S_1}(\theta, s)$$

$$\Delta V_S = V_{S_2}(\theta, s) - V_{S_1}(\theta, s)$$

and $R_{S_1}(\theta, s)$, $R_{S_2}(\theta, s)$ are obtained from Eq. (15').

For white-light measurements it is necessary, therefore, to calculate the white-light reflectance of the two standards and then to measure the irradiance of the light source, $G_S(0^\circ, \lambda) = G_S(\lambda)$.

5. Test of validity

The method has been validated by measurements at $\lambda \approx 650$ nm, using three 1.25 in. in diameter grey diffuse standards from Labsphere: SRS-02-010, SRS-05-010 and SRS-10-010, of nominal reflectance 2%, 5% and 10%, respectively. For the sake of brevity, they are here indicated as S02, S05 and S10, respectively. The total hemispherical reflectance of the three standards, at $\theta = 8^\circ$ and at the different wavelengths, can be obtained by the calibration charts of the samples, that report the reflectance values at 50 nm steps for the 250–2500 nm range. To apply the DRM method, it was necessary to independently measure the reflectance of the standards by using the method described in Refs. [3–5] (see also Section 3). The reflectance, $R_S(\theta, 633$ nm), of the three standards is reported in Fig. 7.

As told in advance at the end of Section 4.1, the angle-resolved reflectance curve of the diffuse gray standards is not flat as should an ideal diffuser be [7]. The reflectance tends to increase with the angle, in a monotonous way. This effect, higher for the darker standards, is resumed in telling that the standard is not a perfect lambertian diffuser. The slightly waving shape of the curves, moreover, is not peculiar of the standards material, as this is made of a homogeneous blend, but should be due, most likely, to the small disturbance produced on the reflected light by the imperfect homogeneity of the internal wall of the sphere. Internally to the

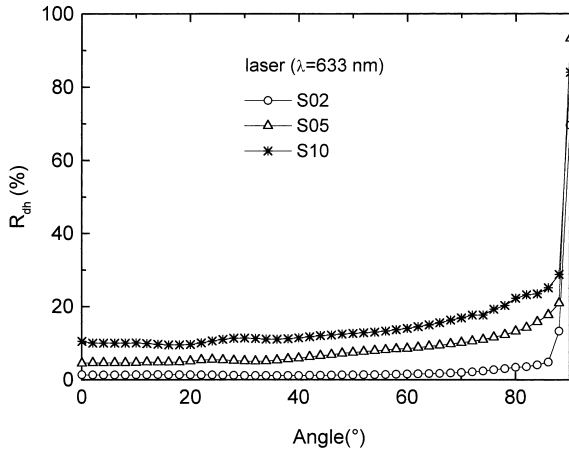


Fig. 7. Total directional/hemispherical reflectance of the three standards: S02, S05 and S10, measured by using a He-Ne laser operating at $\lambda = 633$ nm.

sphere, in fact, the ports slightly absorb the light in correspondence with their border.

The three standards were afterwards characterized by using the DRM apparatus configured as reported in Fig. 5a, provided with a QTH light source and an interference filter of 650-nm nominal central wavelength and 70-nm nominal bandwidth. The spectrum of light at the input of the integrating sphere, as measured by the Oriol spectrograph, is shown in Fig. 8. A lock-in configuration, with a chopping frequency of 70 Hz, was arranged.

Fig. 9 shows the current curves obtained by measuring the three standards by DRM. The current, in this case, corresponds to the signal $V_S(\theta)$ reported in Eq. (7) and following. The current curves show a characteristic behaviour, that is the tendency to grow at increasing θ , the reaching of a maximum at 70–80° and the falling to zero at 90°. This is due to two combined and opposite effects, that is the increase, with θ , of $R_S(\theta)$ (see Fig. 7) and the decrease, with θ , of $\cos \theta$. We have, in fact, from Eq. (7), neglecting the box reflectance:

$$\begin{aligned} V_S(\theta) &\approx kG_0R_S(\theta)S_S(\theta) \\ &= kG_0R_S(\theta)S_S(0^\circ)\cos\theta \\ &= \dots = kG_0S_0[R_S(\theta)\cos\theta] \end{aligned} \quad (19)$$

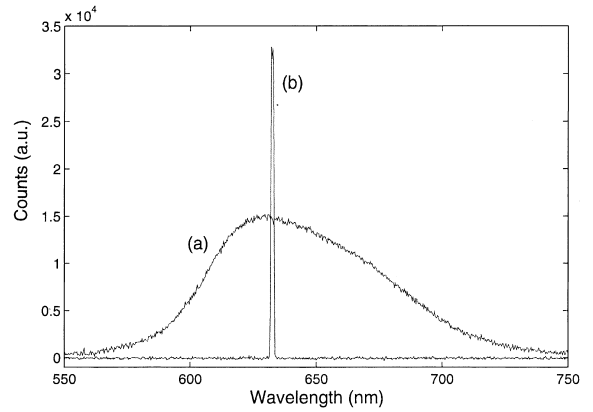


Fig. 8. (a) Spectrum of the light used in the DRM measurements. (b) Line of the He-Ne laser light.

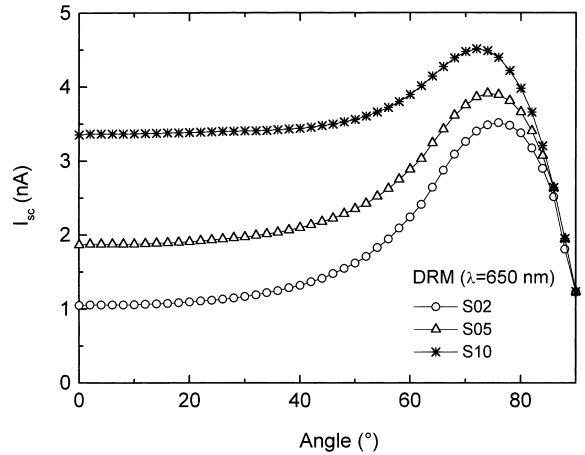


Fig. 9. Current curves of the three standards of Fig. 5, as obtained following the DRM procedure.

It is easily found that the maximum of the $V_S(\theta)$ curve, corresponding to I_{SC} (nA) of Fig. 9, is reached at the angle θ_M satisfying the expression:

$$\operatorname{tg}\theta_M \approx R'_S(\theta)/R_S(\theta) \quad (20)$$

obtained deriving $V_S(\theta)$ and equalizing to zero. $R'_S(\theta)$ is the derivative of $R_S(\theta)$ respect to θ .

The DRM current curves appear very regular, contrary to the laser measurements of Fig. 7. This fact has a double significance. First of all, the DRM measurements seems to be less sensitive to the optical heterogeneity of the neighbouring en-

vironment (the integrating sphere with the multiple ports). Secondly, the measurements seems to be more stable and less affected by statistical fluctuations. This should assure more precise results.

By using the data of current for the S02 and S10 standards and applying Eq. (11'') the reflectance curve for the S05 standard was simulated. It is compared in Fig. 10 with the curve obtained by laser at $\lambda = 633$ nm. The DRM reflectance curve shows a higher regularity than those measured by laser. This confirms the validity of DRM as an alternative, wherever possible, to the old methods.

A comparison between laser and DRM measurements, confined to the 0–80° interval, is also reported in Fig. 11, where the angle-resolved reflectance behaviour of a mono-Si solar cell is shown. Both curves of Fig. 11 show a waving behaviour that should not derive from disturbances by the sphere wall, but most likely are due to the particular type of cell under test. This cell, in fact, is made of a textured surface with square pyramids. Changing the angle θ , in this case, has the effect of changing the incidence angle of the beam on the different facets of the small (≈ 10 μm) pyramids.

The agreement between laser and DRM measurements, as coming from Fig. 10 and particularly from Fig. 11, appears quite good and

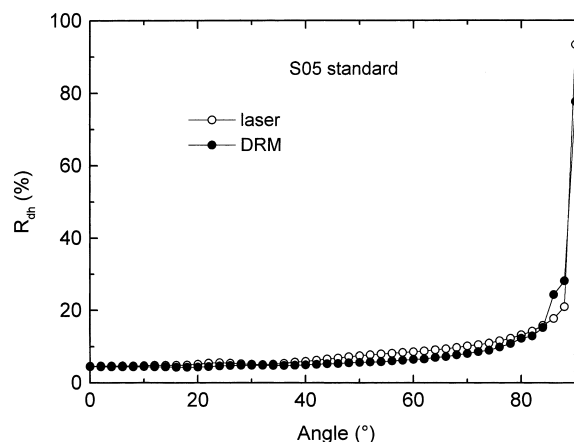


Fig. 10. Comparison between the total directional/hemispherical reflectance of the S05 standard obtained by laser ($\lambda = 633$ nm) and by DRM measurements ($\lambda = 650$ nm).

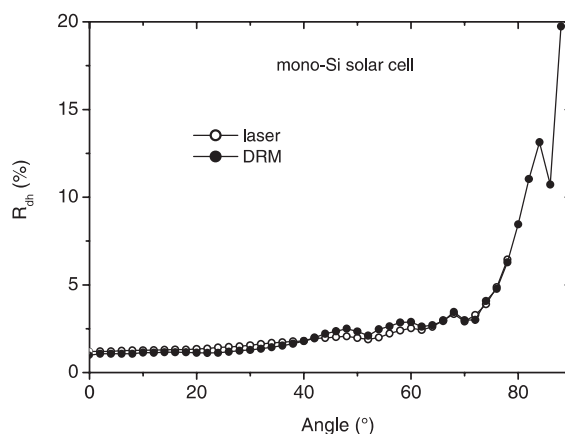


Fig. 11. Comparison, confined to the 0–80° interval, between the directional/hemispherical reflectance of the mono-Si solar cell obtained by laser and by DRM measurements.

represents a positive result for the test of validity of DRM.

The DRM has been applied also to other PV devices. One of these consisted of a m-Si solar cell, textured by a “honeycomb” structure [5,9]. Fig. 12 shows the current curves obtained for the two standards S02 and S10, used as reference, and for the solar cell. Fig. 13 finally shows the DRM reflectance curve at $\lambda \approx 650$ nm obtained for the solar cell applying Eq. (11''). Due to the absence now, on the textured surface, of oriented facets,

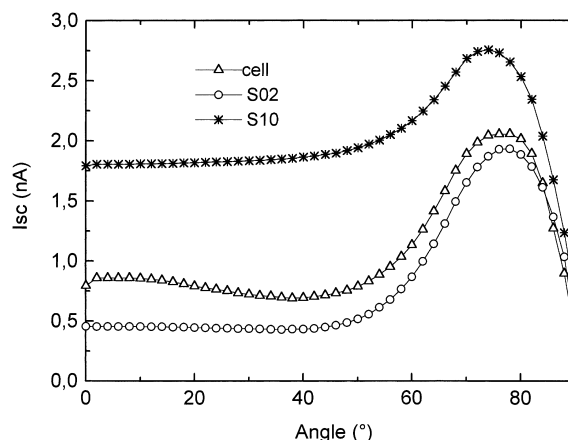


Fig. 12. Current curves for the two standards: S02 and S10, and for the m-Si cell, as obtained following the DRM procedure.

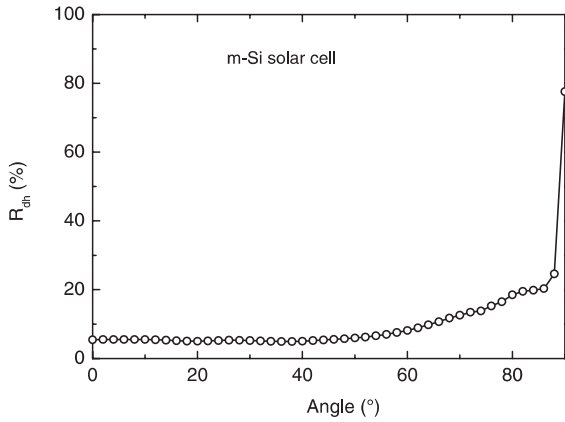


Fig. 13. Directional/hemispherical reflectance of the m-Si solar cell, as obtained by applying the DRM method.

both the current and reflectance curves of the m-Si cell appear very regular (see Figs. 12 and 13).

6. Precision of the method

The presence of the absorber (a) in the sphere can induce a small error in the measurements at high values of θ . As it is shown in Fig. 14a, in fact,

at the angle θ_L the sample front surface starts to see the absorber and a small fraction of the light diffused by the sample is absorbed by (a), and then not measured by (r). It is easily found that:

$$\theta_L = \arccos(D_A/D_S) \quad (21)$$

where D_A and D_S are the diameters of the cylinder's base and of the sphere, respectively. In our measurements, we have $D_A = 4.5$ cm and $D_S = 40$ cm, and the limit angle takes the value $\theta_L \approx 84^\circ$, that is very close to 90° . This portion of light is effectively very small if the sample is a good light diffuser, as the solar cells with textured surfaces, used in this work, are. When dealing with diffusive samples, however, it is expected that the same fraction of reflected light is absorbed by (a) from the sample and from the diffuse reflectance standards, with a minimum impact on the precision of reflectance measurements. The situation changes when dealing with specular samples, for which a new limit angle can be defined. As it is shown in Fig. 14b, in fact, for these type of samples, there is a favourable condition which determines the effective limit angle to be higher than θ_L , and precisely:

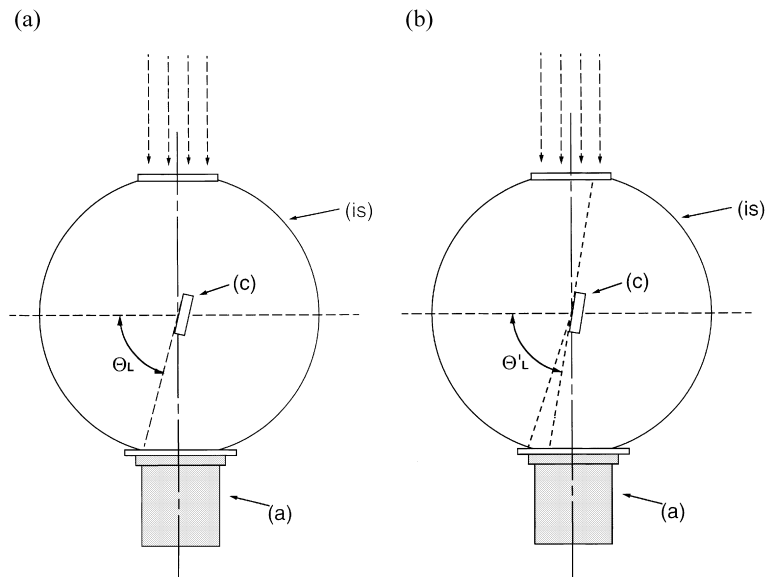


Fig. 14. (a) Schematic of the DRM apparatus with the sample oriented at the limit incidence angle, θ_L . (b) Orientation of a specular sample in correspondence to the angle θ'_L .

$$\begin{aligned}\theta'_L &= \theta_L + \frac{(\pi/2 - \theta_L)}{2} = \theta_L/2 + \pi/4 \\ &= \frac{\arccos(D_A/D_S)}{2} + \pi/4\end{aligned}\quad (21')$$

In the actual case, with $\theta_L \approx 84^\circ$, we find that $\theta'_L \approx 87^\circ$, that is very close to the 90° limit. The discussed error can be definitely minimized by reducing as much as possible D_A respect to D_S . This implies the preparation of a collimated beam, at the input of the sphere, with a section only slightly larger than the box window dimension, and the reduction of the cylinder diameter to a minimum, compatible with the full absorption of the parallel beam when the box is lifted.

There is another potential source of error at high incidence angles, that is the shadowing effect produced on the sample by the front edge of the box window. This error can be reduced making a box with a thinner front face. It could be even completely removed opening a window that suits the shape of both the test sample and the reflectance standard. This condition, however, was not realized in our experiments and it is not easy, anyway, to realize in practice. The influence of the shadowing effect on the precision of measurements is minimized by the fact that the portion of surface shadowed by the box window during measurements is the same for both the unknown sample and for the standards.

The analysis of accuracy of DRM measurements is not straightforward. Due to the lack in literature of calibrated values of angle-resolved diffuse reflectance, in fact, the reflectance curves of the standards ($R_{S_1}(\theta)$ and $R_{S_2}(\theta)$), measured by laser following the old procedure [3–5], represents the only references for our measurements.

The error to be assigned to $R_C(\theta)$, from DRM measurements, derives from the propagation of the errors on three voltage (or current) measurements (V_{S_1}, V_{S_2}, V_C), on two reflectance measurements (R_{S_1}, R_{S_2}) and on the angle θ . Systematic errors on θ have been practically eliminated by calibrating the goniometer, installed on the window (w3), respect to the specular component of the sample reflected beam or respect to the reflected beam of a mirror placed in the box in place of the sample. To have an idea of propagation of errors

from DRM measurements, we have supposed negligible the errors on the reflectance values $R_{S_1}(\theta)$ and $R_{S_2}(\theta)$, which are the references for these measurements. By imposing the (realistic) approximations:

$$R_{S_2}(\theta) \approx 2R_{S_1}(\theta); \quad R_C(\theta) \approx [R_{S_1}(\theta) + R_{S_2}(\theta)]/2 \quad (22)$$

it is found that the relative error on $R_C(\theta)$ can be roughly estimated by the following expression:

$$\Delta R_C(\theta)/R_C(\theta) \approx 6[R_{S_1}(\theta)]^2[\Delta V(\theta)/V_{S_1}(\theta)] \quad (23)$$

from which it comes out that it is a lot smaller than the relative error on the voltage (or current) measurements, when a value of $R_{S_1}(\theta) \approx 5 \times 10^{-2}$ is used (see Fig. 7). The difference found between laser and DRM measurements (Figs. 10 and 11) can be only explained as due to systematic errors in the measurements, like those discussed previously.

7. Conclusions

A new method for measuring the directional/hemispherical reflectance of a flat sample surface has been presented. The method is based on differencing measurements carried out on the sample under test and on two standards of diffuse reflectance. Due to the differencing procedure followed to obtain the unknown reflectance, the method has been named DRM. It permits, in principle, to carry out measurements of total hemispherical reflectance at continuously variable angle of incidence, in the full range $0-90^\circ$. Due to the homogeneous illumination, at any angle, of the selected area of the sample, the method proves to be particularly suitable for measuring optically heterogeneous samples, as PV materials and devices generally are. A relevant practical advantage of the method is the possibility to carry out spectral measurements at high incidence angles in a very simple way. Traditional methods require, on the contrary, the use of lasers or sophisticated optical apparatuses.

Respect to the traditional methods, DRM shows a low sensitivity to the optical homogeneity

of the environment (the integrating sphere) and, as a consequence, the current and relative reflectance curves show a high degree of regularity.

Acknowledgements

The authors acknowledge H. Yakubu and R. De Rosa for the help received in the preparation of the samples and S. Ferlito for the set-up of spectral measurements. They also acknowledge G. Scaglia (LOT Oriel, Italia) for helpful discussions. The authors thank also J. Zhao and A. Wang of the Photovoltaic Special Research Centre of the University of New South Wales, Sydney, for the supply of the solar cells. This work was done with the financial support of the Italian Ministry of University and Technological Research (MURST).

References

- [1] IEC Standards 891 and 1215, Bureau Central de la Commission Electrotechnique Internationale, Genève.
- [2] ASTM, Designation E 1175 – 87 (Reapproved 1996), Standard test method for determining solar or photopic reflectance, transmittance, and absorptance of materials using a large diameter integrating sphere.
- [3] A. Parretta, Patent It. A.N. RM 97 A 000676, 5 November 1997.
- [4] A. Parretta, A. Sarno, H. Yakubu, *Opt. Commun.* 161 (1999) 297–309.
- [5] A. Parretta, A. Sarno, P. Tortora, H. Yakubu, P. Maddalena, J. Zhao, A. Wang, *Opt. Commun.* 172 (1999) 139–151.
- [6] A. Parretta, A. Sarno, P. Tortora, Patent It. A.N. RM 99 A 000656, 25 October 1999.
- [7] G. Kortum, *Reflectance spectroscopy, principles, methods, applications*, Springer, Berlin, 1969, p. 28.
- [8] P. Maddalena, A. Parretta, P. Tortora, *Opt. Commun.*, submitted for publication.
- [9] J. Zhao, A. Wang, M.A. Green, F. Ferrazza, *Appl. Phys. Lett.* 73 (1998) 1991–1993.